

Abstract.

With IMF B_z strong and positive (northward), strong sunward convection may develop in the central polar cap with return flows poleward of the usual auroral oval (NBZ conditions). The NBZ sunward convection maximises close to local noon at latitudes between the cusp and the magnetic pole (e.g., *Stauning et al., 2002*). In addition to depending on the strength of IMF B_z , the reverse convection intensities relate to the ionospheric conditions, in particular, the conductivity varying with local time, season and solar cycle, and to the geomagnetic field configuration. The immediate effect of reverse convection is to give negative PC index values. However, inclusion of reverse convection events in the data base used to derive index coefficients has adverse consequences for the quality of the PC indices by adding the dependencies of NBZ events to the index values and enhance saturation effects.

Satellite observations of NBZ conditions

From MAGSAT and Ørsted satellites (*Stauning, 2002*), the horizontal magnetic vectors were measured at positions covering the northern as well as the southern polar caps. The internal field as well as the ring current contributions were subtracted from the measured values, which were then sorted within narrow bins of seasonal, solar wind, and interplanetary magnetic field (IMF) conditions. With bi-variate interpolation (*Akima, 1978*), the result for the "Z3SS" case ($-10 < \text{IMF } B_x < +10$, $-3 < \text{IMF } B_y < +3$, $+5 < \text{IMF } B_z < +10$ nT, southern summer) is displayed in Fig. 1.

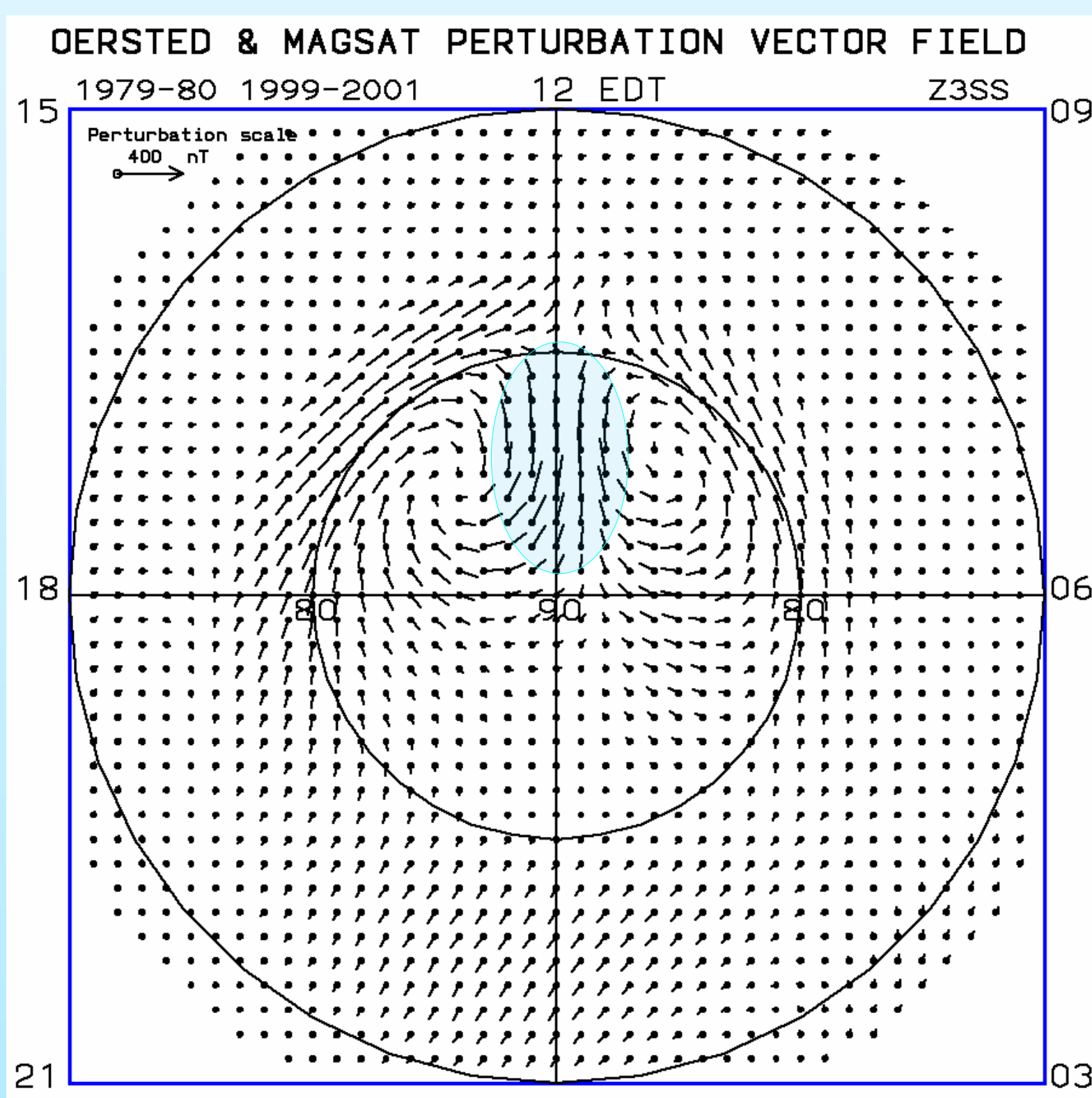


Fig. 1. Reverse convection case Z3SS. Convection vectors are formed by rotating magnetic perturbation vectors by 90°. The region of strong transpolar reverse convection has been emphasized. This region is positioned near noon in eccentric dipole time (EDT) and between 80° and 90° EDT latitudes (i.e. between Cusp and geomagnetic Pole). (from *Stauning, 2002*)

Ground observations of NBZ conditions

At groundbased magnetic observations the NBZ conditions imply negative values of the magnetic variations when projected to the "optimum direction" considered to be perpendicular to the dominant DP2 forward convection direction. The effects are seen by comparing four widely used PC index versions: OMNI (*Vennerstrøm, 1991*), AARI (*Troshichev et al., 2006*), IAGA-endorsed (*Troshichev 2011*), and DMI (*Stauning, 2016*).

Version	Epoch scaling	Solar activity	Reverse convection	Reference level
OMNI	1977-1980	Peak of cycle	Frequent	BL, No QDC
AARI	1998-2001	Peak of cycle	Frequent	BL and QDC*
IAGA	1997-2009	Cycle average	Average	BL and QDC**
DMI	1997-2009	Cycle average	Excluded	BL and QDC***

BL: Base Level. QDC: Quiet Day Curve (Quiet daily variation not related to E_{KR})
QDC*: based on running 30 days quiet samples (*Janzhura & Troshichev, 2008*)
QDC**: running 30 days quiet samples + solar wind sector contribution (*Janzhura & Troshichev, 2011*)
QDC***: 40 days solar rotation weighted quiet samples (*Stauning, 2011*)

PC index basics.

The assumed relation between polar cap horizontal magnetic field variations projected to an "optimal direction", considered to be perpendicular to the DP2 transpolar plasma flow, and the Kan and Lee (1979) merging electric field ($E_M = V_{SW} \cdot B_T \cdot \sin^2(\theta/2)$) has the form:

$$\Delta F_{PROJ} = \alpha \cdot E_M + \beta \quad (1)$$

where α is the "slope" (e.g. in units of nT/(mV/m)), while β (e.g., in units of nT) is the "intercept". The calibration parameters are calculated by regression from cases of measured values through an extended epoch. From equivalence with E_M , the Polar Cap Index PC is defined by:

$$PC = (\Delta F_{PROJ} - \beta) / \alpha \quad (2)$$

The optimal direction is found by varying its angle, ϕ , with the EW meridian to maximise the correlation between ΔF_{PROJ} and E_M

Reverse convection properties at different locations

Figs. 2a-c display reverse convection intensities at Thule (Qaanaaq) and Resolute Bay in the northern polar cap, and Vostok and Concordia Dome C in the southern polar cap. Reverse convection intensities are measured through the number of hours with $\Delta F_{PROJ} < -50$ nT.

Thule, Resolute and Vostok are all close to the latitude of maximum reverse convection in Fig. 1, while Dome C is located close to the geomagnetic (CGM) pole. Noon at local solar time (LT) and magnetic local time (MLT) are close at Thule and Resolute, but quite different at Vostok.

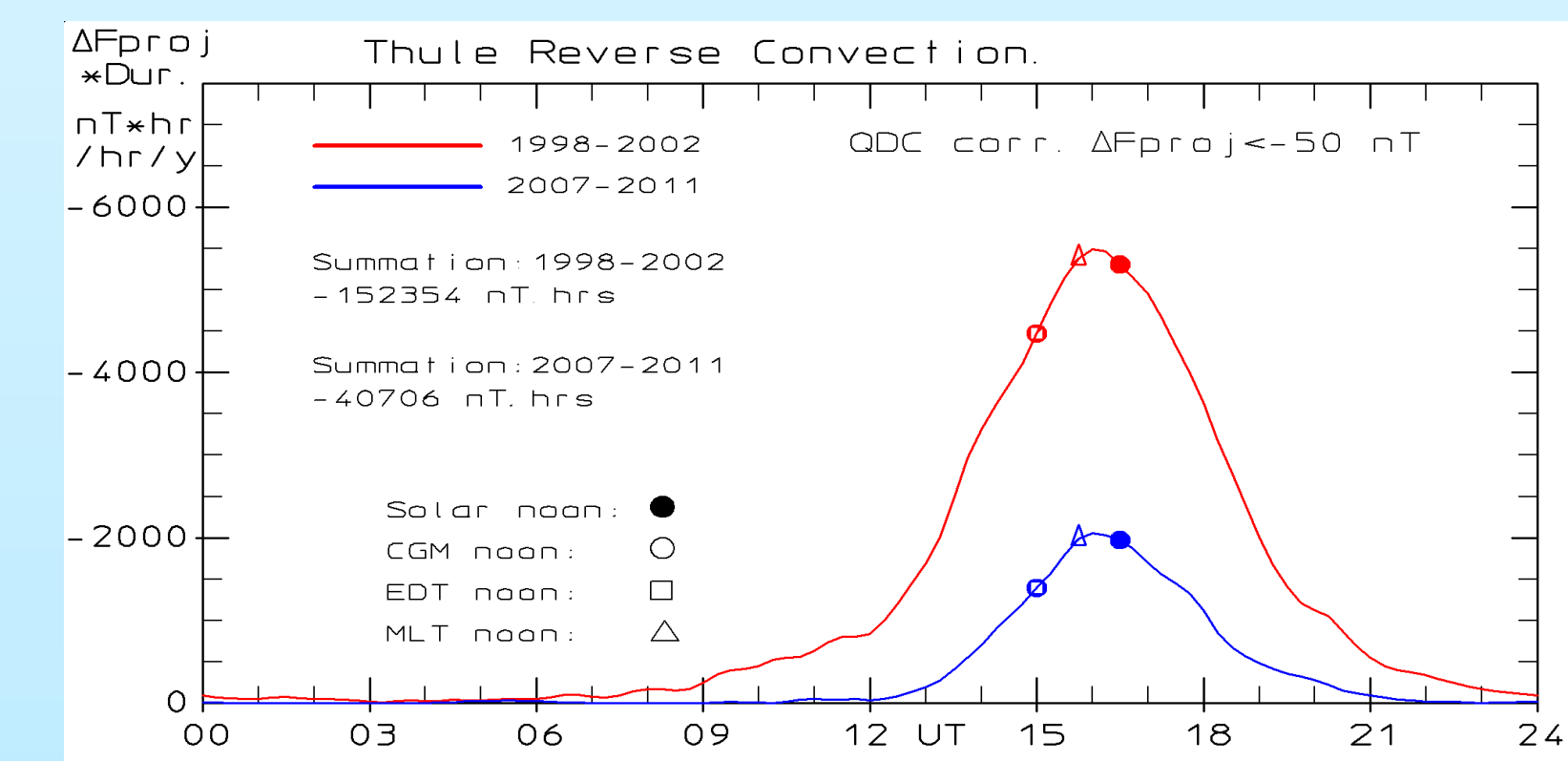


Fig. 2a. Thule
Geogr. Lat. Lon:
77.48°, 290.83°
CGM Lat. Lon.:
85.29°, 31.30°
LT=00 at 04.61 UT
MLT=00, 03.05 UT

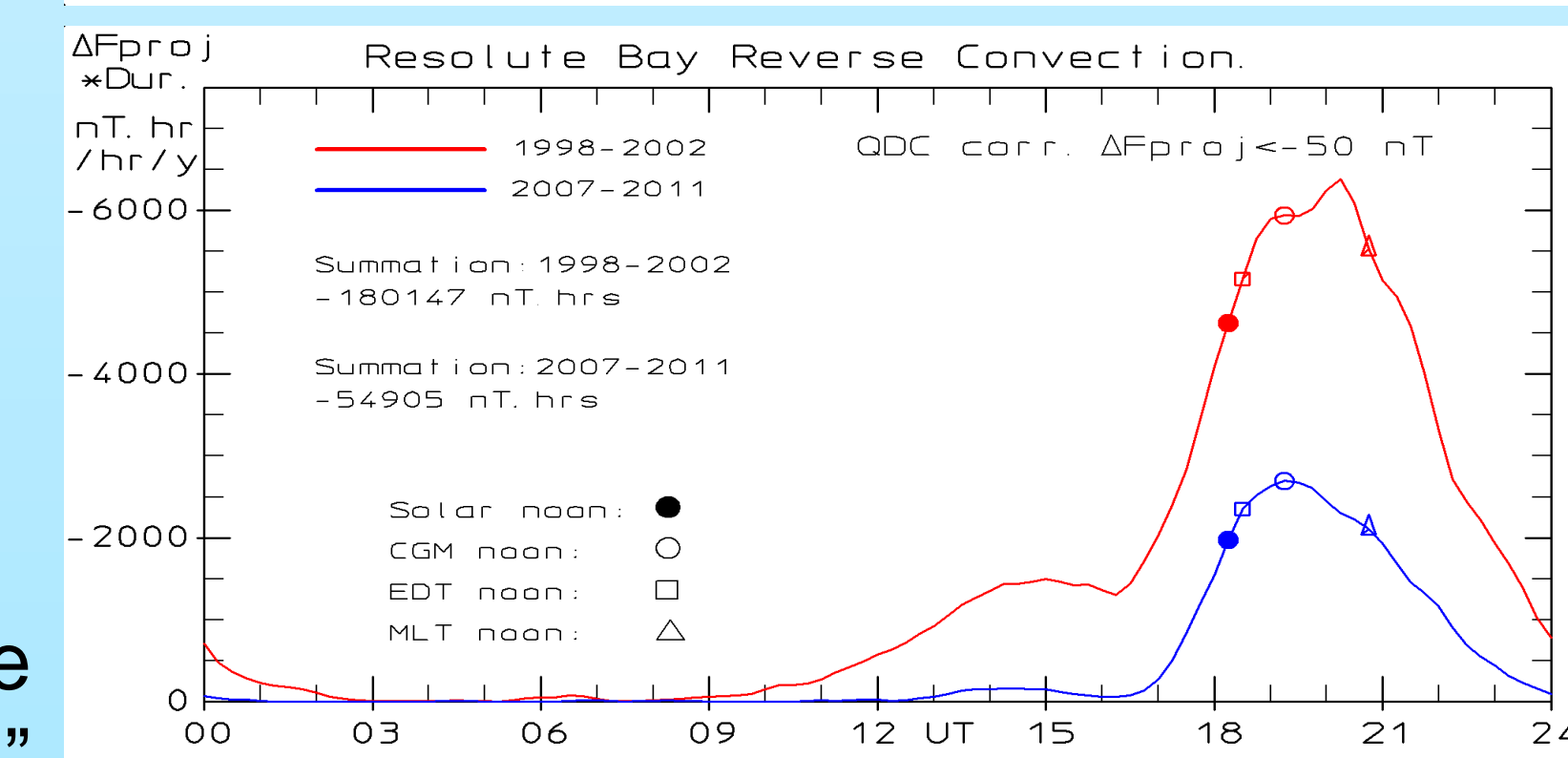


Fig. 2b. Resolute
Geogr. Lat. Lon:
74.68°, 265.10°
CGM Lat. Lon.:
83.27°, 319.40°
LT=00 at 06.33 UT
MLT=00, 07.28 UT

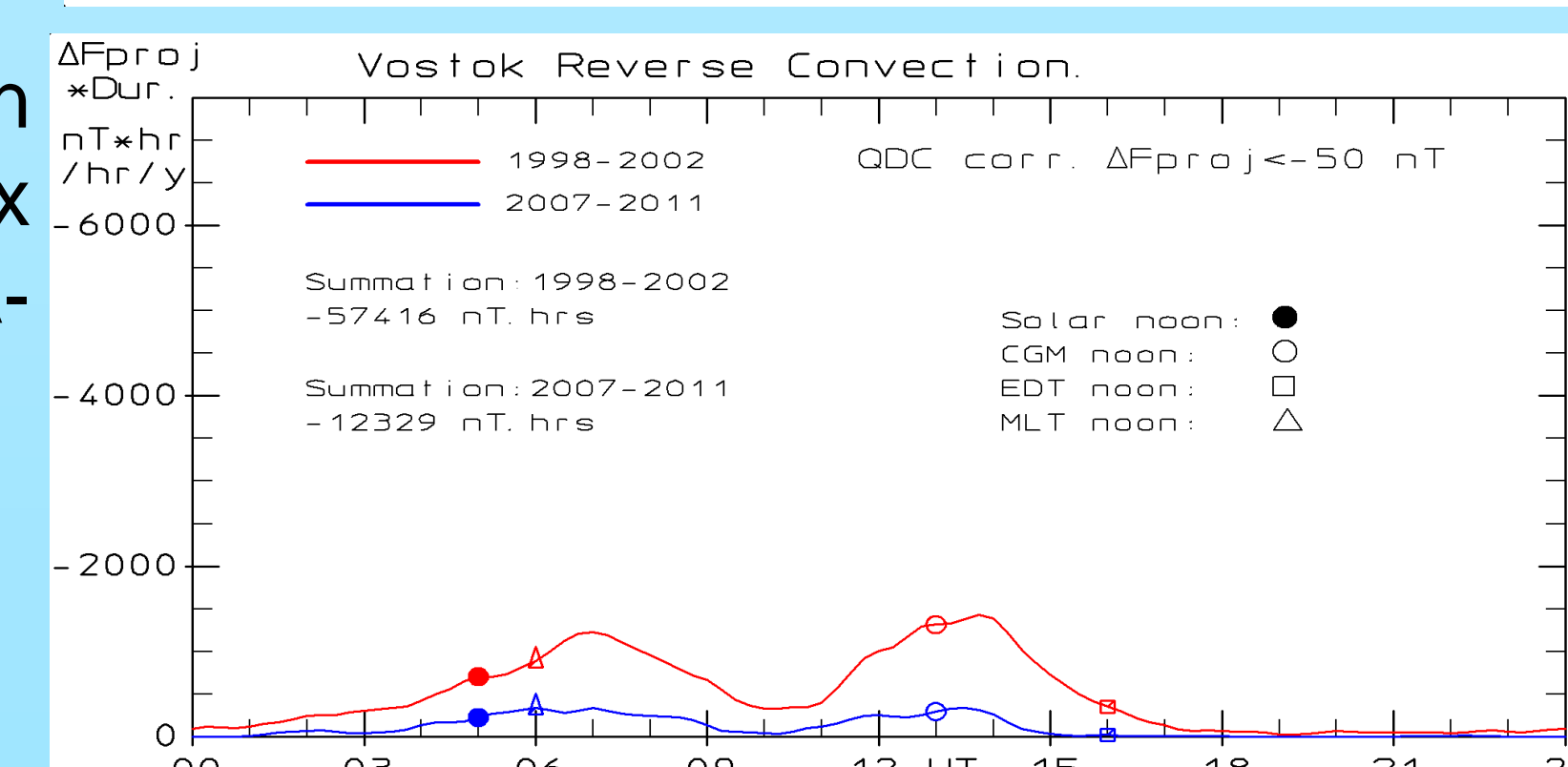


Fig. 2c. Vostok
Geogr. Lat. Lon:
-78.46°, 106.84°
CGM Lat. Lon.:
-83.57°, 54.80°
LT=00 at 16.88 UT
MLT=00, 01.02 UT

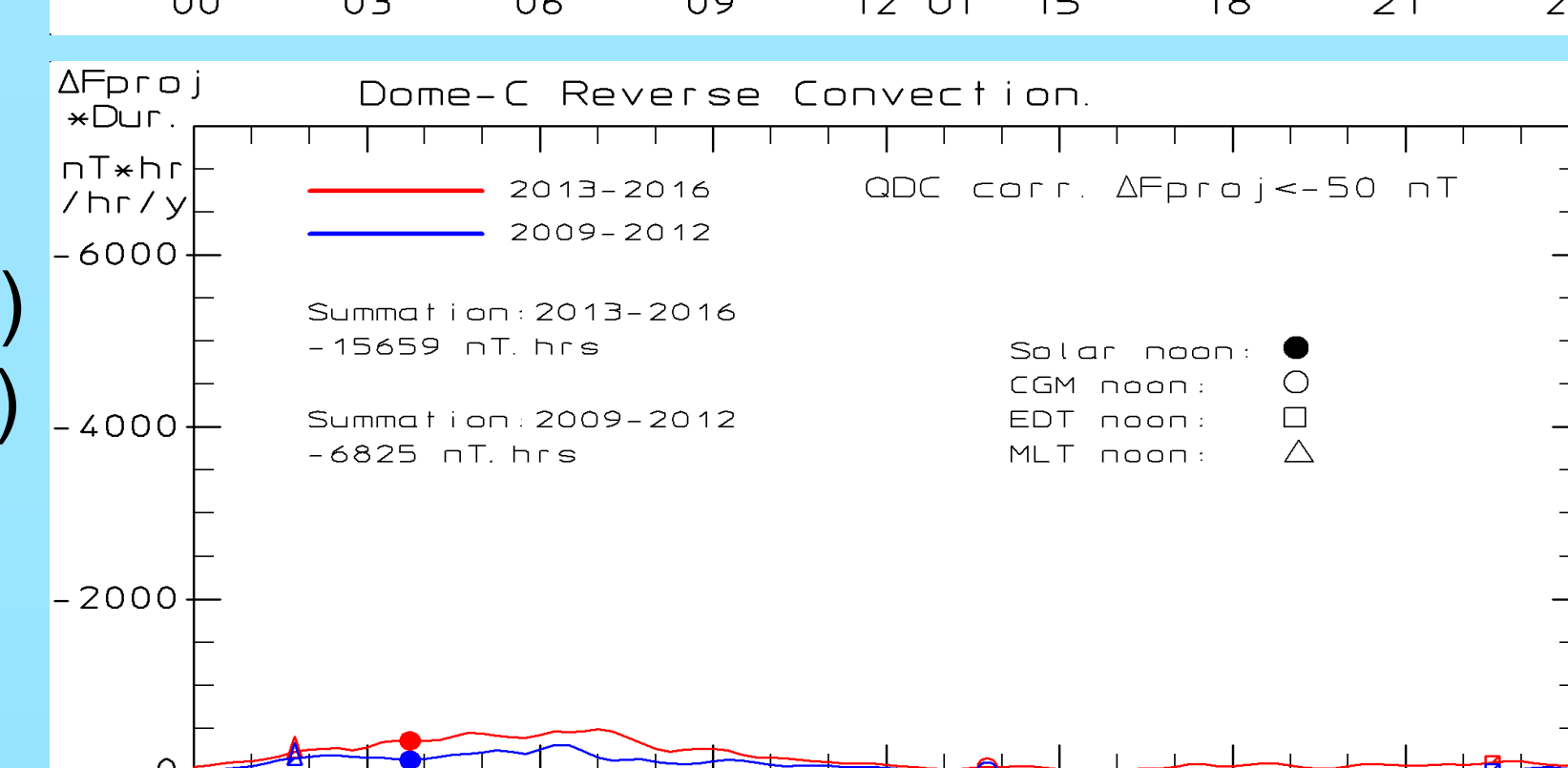
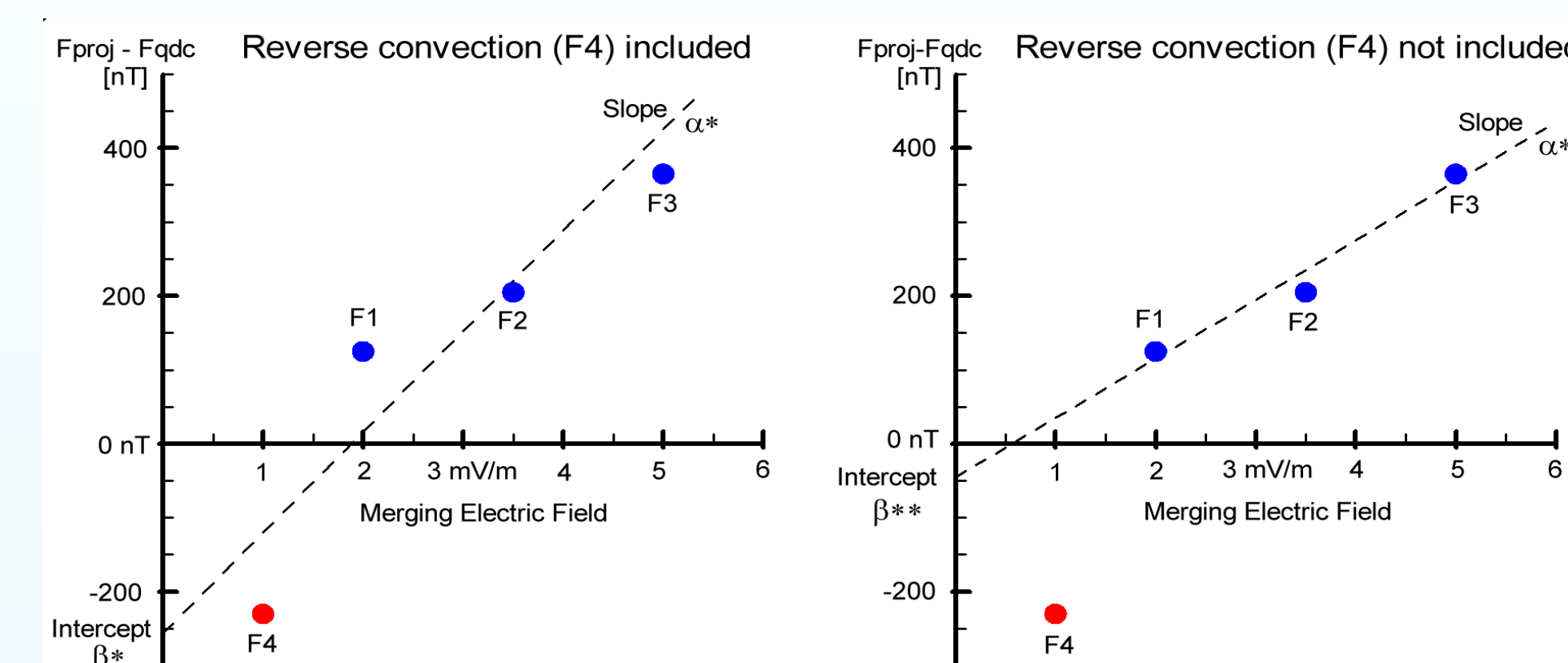


Fig. 2d. Dome C
Geogr. Lat. Lon:
-75.25°, 124.17°
CGM Lat. Lon.:
-88.81°, 43.07°
LT=00 at 15.72 UT
MLT=00, 01.86 UT

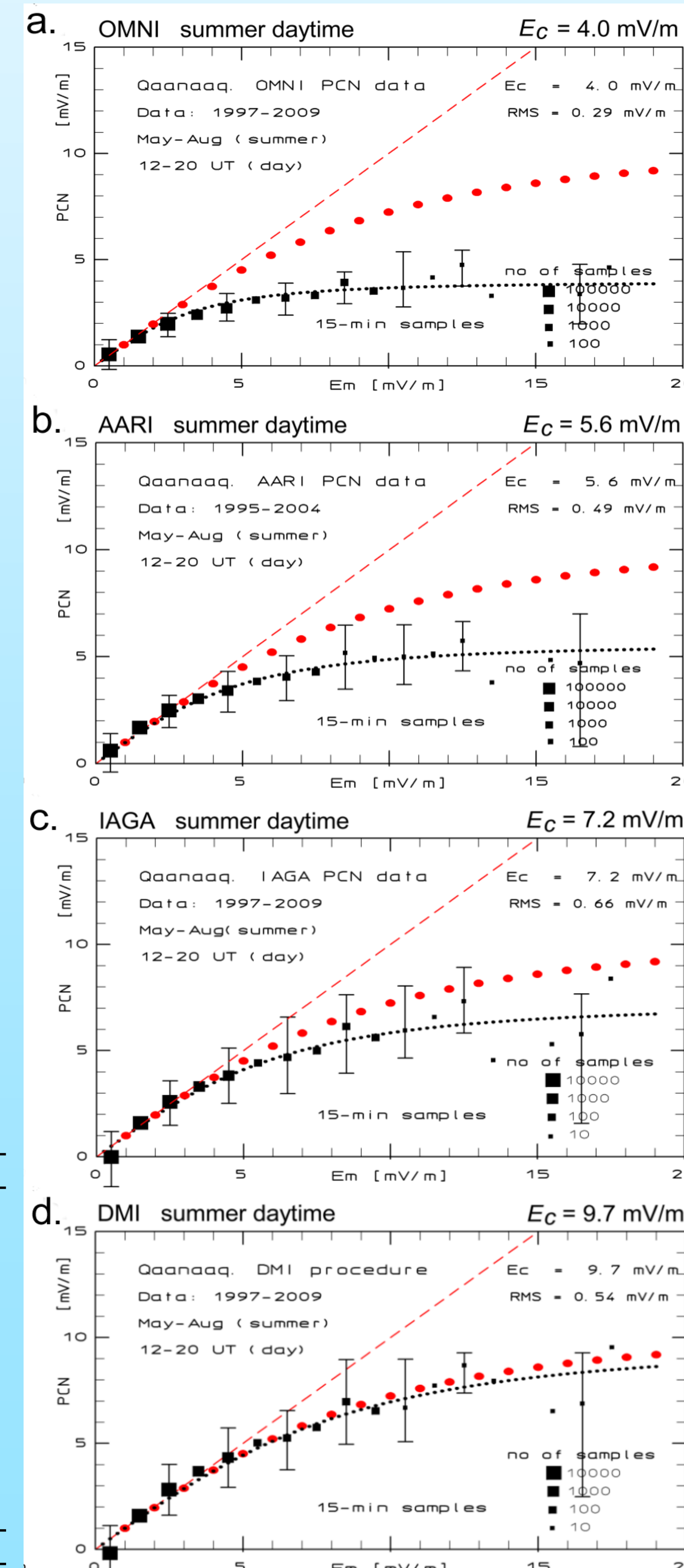
Reverse convection effects on PC indices

Fig. 3. (a) Reverse convection case, red point F4, ($\Delta F_{PROJ} < 0$) is included in the regression. (b) Regression based on forward convection cases ($\Delta F_{PROJ} > 0$) only. Note larger slope and more negative intercept in (a) compared to (b). (From *Stauning, 2013*)



The effects from the varying relative amount of reverse convection samples included in the regression to derive slope and intercept is seen in Fig. 4. The OMNI version has the largest slopes and also the most negative intercept values taking into account that the QDC is not included in the quiet reference level (QL).

Fig. 5.



The diagrams of Fig. 5 display for summer daytime conditions and for each of the PC index versions the relations between bin-average PCN index values (black squares) and values of the merging electric field, E_M . The amount of samples within each unit of E_M is indicated by the size of the squares on the scale shown in the lower right part of the field. The dashed line indicates equality. The reference curve indicated by the large red dots is based on least squares fit to the relation in Eq. 3 between samples of PC and E_M observed during magnetic storm events (*Stauning, 2012*).

$$PC = E_M / (1 + (E_M / E_C)^2)^{1/2} \quad (3)$$

with $E_C = 10.5$ mV/m). The curve of small dots indicates the best fit of the form of Eq. 3, but with variable E_C , to the PCN bin averages. In the corresponding diagrams for winter night samples, the best fit curve in all index versions approximates the reference curve. The figure indicate saturation of the PC indices in all versions. The 50% saturation ($PC = 0.5 \cdot E_M$) level is reached at $E_M = \sqrt{3} \cdot E_C$.

Part of the saturation effect is caused by the transition between the merging electric field in the solar wind and the cross polar cap electric field. In the *Kivelson-Ridley (2008)* model the transition is controlled by the Alfvénic conductivity, Σ_A in the solar wind and the polar cap ionospheric conductivity, Σ_P , according to:

$$E_{KR} = E_M \cdot 2 \cdot \Sigma_A / (\Sigma_P + \Sigma_A) \quad (4)$$

Using E_{KR} instead of E_M in the displays removes most of the saturation trend in the DMI version and makes the average samples closely approach the dashed line of equality. For the other versions, the remaining amount of saturation is mainly caused by the effects of reverse convection events on the calibration parameters. The "OMNI" version (*Vennerstrøm, 1991*) performs worst. The epoch of data (1977-1980) used for derivation of calibration parameters in this version has the highest relative amount of reverse convection cases. The "AARI" and "IAGA" versions perform in-between.

Conclusions

- The NBZ reverse convection samples, when included in the regression calculations, transfer their narrow distributions with location within the polar cap, season, and local time to the derived calibration parameters and further onward to the PC indices.
- For summer daytime samples, the 50% saturation level is reached at $E_M = 6.0$ mV/m for the OMNI version, 9.7 mV/m for the AARI, 12.5 mV/m for the IAGA, and 16.8 mV/m for the DMI version. The differences in saturation properties mainly relate to the relative amount of reverse convection samples in the data base used for parameter calculations.
- The calculation methods used for the IAGA-endorsed version should be modified to omit reverse convection samples from the calculations of calibration parameters.